

Investigation of Compressible Viscous Flows over Open Cavities Including the Effects of Shear Layer Thickness and Multiple Deck Structure on Interaction with the Trailing Edge

A.B. Rahimi¹

The problem considered in this paper is that of compressible viscous flow over an open rectangular cavity, including the effects of shear layer thickness and triple deck structure on interaction with the trailing edge. This analysis unifies analytical cavity studies and provides a wave-number correction for the method of Tam and Block [1], which studies the case of a compressible inviscid flow with a constant shear layer thickness spanning an open cavity. Here, basic equations for a two-dimensional compressible viscous flow are derived. The effect of non-parallelism of the mean flow is introduced. This weakly non-parallel mean flow is perturbed to obtain the governing equations for the shear layer. The inverse of the Reynolds number, here related to the weak effect of non-parallelism of the mean flow, serves as a perturbation parameter. The shear layer is divided into a region of inviscid flow away from the trailing edge and a region where viscous effects are important, near the trailing edge, as a typical boundary layer problem. The viscous region is analyzed by proper scaling of the independent variables. Distinguished limits are obtained by balancing the terms in the set of the governing equations. A multiple deck structure, containing three distinct regions, occurs, each region with a different scaling. Normal modes for the flow properties are introduced to predict an eigenvalue problem, which governs the wave-number/frequency relationship in each deck, as well as the inviscid region. These eigenvalue problems are derived using the Fredholm Alternative and are solved numerically by use of a fourth-order Runge-Kutta method. The method of asymptotic expansions is used to match these wave numbers to those among the multiple deck structure, as well as to the one for the inviscid region. This wave-number, uniformly valid throughout the region, is used as a correction to the one derived by Tam and Block. This study proves that by considering the effect of non-parallelism of the mean flow, a lower wave-number/frequency is produced at any spanwise location for a given excitation frequency. Predicted discrete tone frequencies, based on this corrected value of wave-number, produce a closer agreement with the experimental results.

INTRODUCTION

The problem considered herein is that of a two-dimensional compressible viscous flow over an open cavity. The problem is considered from a rigorous mathematical viewpoint. This is to include the effect of shear layer thickness variations along the span of the cavity and the enforcing of the boundary conditions

at the trailing edge. In terms of the modeling of Tam and Block [1], a feedback mechanism occurs, due to the deflection of the shear layer into a cavity. Reflected waves excite the shear layer (see Figure 1). In developing this feedback model, Tam and Block assumed that the rectangular cavity was two-dimensional and that the mean flow inside the cavity could be ignored. They, as evidenced by flow visualization, proposed that the shear layer oscillates up and down near the trailing edge of the cavity. During the upward motion of the cycle, the fluid of the shear

1. Department of Engineering, Ferdowsi University of Mashhad, P.O. Box 91775-1111, Mashhad, I.R. Iran.

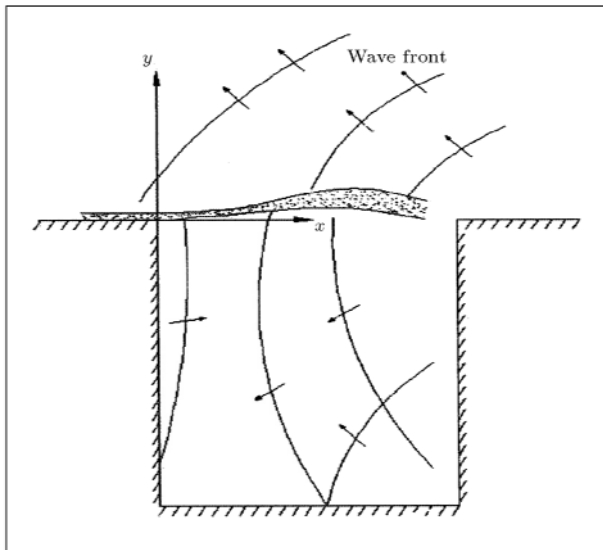


Figure 1. Shear layer modeling.

layer shields the trailing edge of the cavity from the external flow. Under this circumstance, the external fluid flows smoothly over the trailing edge and no pressure waves of any significance are generated. When the shear layer is deflecting downward, there is an inflow of external fluid into the cavity. A high-pressure region forms momentarily near the trailing edge of the cavity. The transient nature of the flow causes the emission of a compression wave. This compression wave propagates in all directions and results in the setting up of a feedback mechanism. The problem of a compressible flow over an open cavity is one of great practical importance. Examples of such flows are those over aircraft wheel wells and weapons bays. Bartel and McAvoy [2] experimentally measured sound pressure levels as high as 170 dB in a weapons bay environment. Levels this high can lead to structural failure and will cause extreme personal discomfort. Thus, methods of reducing sound pressure levels are of the utmost importance. The first step in this reduction is to obtain a useful analytical model of the compressible flow over an open cavity. Besides, the authors motivation is to unify an analytical theory of open cavity flows.

Open cavity flows have been investigated analytically and experimentally. However, many analytical models have severe limitations on their range of application or do not match experimental data. Some of the best analytical models are, in fact, semi-empirical. Krishnamurty [3] performed one of the first experimental investigations in a simulated weapons bay. He showed that an intense, high-frequency acoustic radiation is an essential feature of the problem. The character of the acoustic field was found to depend upon the type of boundary layer, the gap dimensions and the free-stream velocity or Mach number. These results have been

verified by other people, including Gibson [4], Spee [5], East [6] and Smith and Shaw [7], among others. The first significant analytical study of open cavity flows was that of Plumblee, Gibson and Lassiter [8]. They developed a theory for the resonant frequencies and pressure amplifications of a rectangular cavity of arbitrary dimensions in a flow field and derived radiation impedance at all Mach numbers, using the concepts of retarded potential theory, assuming this radiation impedance to be that of a rectangular piston set in a flat wall, which was very large in respect to the dimensions of the piston. Rossiter [9] concluded that it would appear that acoustic resonance does play an important part in determining the frequency and magnitude of the pressure fluctuations, but, the forcing function is a property of the flow over the cavity rather than of the boundary layer approaching it. Smith and Shaw [10] and Bartel and McAvoy [2] have developed semi-empirical models of open cavity flows based upon their experimental observations. These models do reflect the data obtained by the respective investigators, but, are limited to very low Mach numbers. Covert [11] studied cavity behavior by a simultaneous solution of the flow process for the external and internal flows. He assumed the fluid to be inviscid and perfect and argued that the normal velocity and the pressure are continuous across the interface but the tangential velocity may be discontinuous across the cavity interface, hence, a vortex sheet model seemed to be reasonable. Bilanin and Covert [12] developed an analytical model of a shallow cavity using an acoustic monopole to model the trailing edge behavior. Their model is based upon a feedback mechanism first proposed by Rossiter [9], where the pressure field of the monopole drives the shear layer. Block [13] extended the work of Bilanin and Covert to include effects of length-to-depth ratio. To meet the boundary conditions on the internal cavity walls, image sources were used. The appropriate trailing edge behavior has created some controversy. Heller and Bliss [14] studied a water table simulation, which revealed that unsteady motion of the shear layer led to periodic mass addition and removal of the cavity trailing edge. Tam and Block [1], in a study directed toward open wheel well noise, analyzed the open cavity problem using a feedback model, mentioned previously, significantly different from that of Bilanin and Covert. The work of Tam and Block is important because it was the only analytical cavity study to include shear layer thickness effects prior to the study of Kelly [15]. Tam and Block derived an eigenvalue problem for pressure amplitude from which the value of wave-number frequency was produced. The only other analytical studies of the shear layer spanning an open cavity, which includes thickness effects, are those by Kelly and Kelly and LaRose [15,16]. These works were based upon Tam's analysis. What is lacking in

these studies is consideration of the viscosity of the fluid flow. All the other works in this subject are numerical (e.g. [17-23]) or use computer codes (e.g. [24-26]).

In the present work, the main goal is to provide a correction, in terms of the wave-number/frequency, to the technique of Tam and Block, to account for varying shear layer thickness effects and consideration of viscosity in the vicinity of the trailing edge. The problem formulation is started with derivation of the basic field equations for a two-dimensional compressible viscous flow. The effect of non-parallelism of the mean flow is introduced in [27]. This weakly non-parallel mean flow is perturbed to obtain the governing equations for the shear layer. In free shear flows, the viscosity effects can be neglected, as long as no walls are present. Therefore, the flow spanning the cavity away from the trailing edge can be considered inviscid. The effect of viscosity is most important in the vicinity of the trailing edge of the cavity where the shear layer is impinging. Thus, the shear layer can be divided into a region of inviscid flow away from the trailing edge and a region where viscous effects are important, near the trailing edge, as in a typical boundary layer problem. The inverse of the Reynolds number of shear layer flow serves as a perturbation parameter. The weak effect of non-parallelism of the mean flow is related to this parameter. The governing equations for the inviscid region are obtained by neglecting the effect of viscosity. In the vicinity of the trailing edge, the viscous terms are retained. To analyze the viscous region, the independent variables are scaled properly into a set of independent variables magnifying this region. Distinguished limits are obtained by balancing each term with the rest of the terms in the set of the governing equations. Three regions of importance stand out, each identified by a different set of governing equations. This is the multiple deck situation, which can be, and is, used when inviscid and viscous regions in fluid dynamics problems interact [28]. The multiple decks mentioned above are named the fully viscous upper and lower decks, the two located at the trailing edge of the cavity. The other deck situated in between the trailing edge and the inviscid region is named as the outer viscous region. Normal modes for the flow properties are introduced to predict an eigenvalue problem, which governs the wave-number/frequency relationship in each deck. These eigenvalue problems are derived using the Fredholm alternative [29], and solved by numerical techniques. The method of matched asymptotic expansions is used to match these wave-numbers to those among the multiple decks in the viscous region in both directions, as well as to the one for the inviscid region. In this process of matching, the boundary conditions at the trailing edge are enforced. The calculated wave-number of this

analysis serves as a correction to the one obtained by Tam and Block.

PROBLEM FORMULATION

The basic field equations written out in the Cartesian coordinate systems for a two-dimensional viscous, non-conducting, compressible flow with no body force in dimensionless quantities for mass, x -momentum, y -momentum, energy and state, respectively, are:

$$\frac{\partial \rho}{\partial t} + \frac{\partial}{\partial x}(\rho u) + \frac{\partial}{\partial y}(\rho v) = 0, \quad (1)$$

$$\rho \left(\frac{\partial u}{\partial t} + u \frac{\partial u}{\partial x} + v \frac{\partial u}{\partial y} \right) = \frac{\partial p}{\partial x} + \frac{1}{3\text{Re}} \left(4 \frac{\partial^2 u}{\partial x^2} + \frac{\partial^2 v}{\partial x \partial y} - 2 \frac{\partial^2 u}{\partial x \partial y} + 3 \frac{\partial^2 u}{\partial y^2} - 2 \frac{\partial^2 v}{\partial y^2} \right), \quad (2)$$

$$\rho \left(\frac{\partial v}{\partial t} + u \frac{\partial v}{\partial x} + v \frac{\partial v}{\partial y} \right) = \frac{\partial p}{\partial y} + \frac{1}{3\text{Re}} \left(2 \frac{\partial^2 u}{\partial x^2} + 3 \frac{\partial^2 v}{\partial x^2} + \frac{\partial^2 u}{\partial x \partial y} - 2 \frac{\partial^2 v}{\partial x \partial y} + 4 \frac{\partial^2 v}{\partial y^2} \right), \quad (3)$$

$$\rho \left(\frac{\partial T}{\partial t} + u \frac{\partial T}{\partial x} + v \frac{\partial T}{\partial y} \right) = (\gamma - 1) M^2 \left(\frac{\partial p}{\partial t} + u \frac{\partial p}{\partial x} + v \frac{\partial p}{\partial y} \right) + \frac{(\gamma - 1) M^2}{\text{Re}} \left[2 \left(\frac{\partial u}{\partial x} \right)^2 + 2 \left(\frac{\partial u}{\partial y} \right)^2 + \left(\frac{\partial u}{\partial y} + \frac{\partial v}{\partial x} \right)^2 - \frac{2}{3} \left(\frac{\partial u}{\partial y} + \frac{\partial v}{\partial x} \right) \left(\frac{\partial u}{\partial x} + \frac{\partial v}{\partial y} \right) - \frac{2}{3} \left(\frac{\partial u}{\partial x} + \frac{\partial v}{\partial y} \right)^2 \right], \quad (4)$$

$$p = \frac{\rho T}{\gamma M^2}. \quad (5)$$

Here, x and y are the axes of the Cartesian coordinate system, t is time, u and v are components of the flow velocity in the directions of x and y , respectively, ρ is the flow density, p is pressure and T is the temperature of the flow, γ is the ratio of specific heat and Re is the Reynolds number of the shear layer flow. The mean

flow is assumed to be a steady two-dimensional flow with quantities (U, V, P, R, T) satisfying the same set of equations as above without the time-dependent terms and R is mean flow density.

Because the shear layer is assumed to grow in a downstream direction, the mean flow is non-parallel. This non-parallel effect is assumed to be weak and can be represented by a small non-dimensional parameter, ε , which represents the amplitude of growth of the shear layer thickness. That is, whenever x appears in the mean flow quantities, it appears in combination with ε as εx . In addition, the non-parallel component of velocity, V , must be of order ε , while all other mean flow quantities are of order one. Thus, it is consistent to introduce a slow scale defined by:

$$x_1 = \varepsilon x, \quad (6)$$

then, all mean flow quantities are written as functions of x_1 and y . From these equations, it is indeed apparent that:

$$\begin{aligned} U &= O(1), & R &= O(1), & V &= O(\varepsilon), \\ \frac{\partial P}{\partial y} &= O(\varepsilon^2), & \frac{\partial T}{\partial x_1} &= O(1), & \frac{\partial T}{\partial y} &= O(1), \\ 1/\text{Re} &= O(\varepsilon). \end{aligned} \quad (7)$$

The flow variables in the shear layer are assumed to be the mean flow component plus a perturbation quantity. Thus:

$$\begin{aligned} u(x_1, y, t) &= U(x_1, y) + \tilde{u}(x_1, y, t), \\ v(x_1, y, t) &= V(x_1, y) + \tilde{v}(x_1, y, t), \\ \rho(x_1, y, t) &= R(x_1, y) + \tilde{\rho}(x_1, y, t), \\ p(x_1, y, t) &= P(x_1, y) + \tilde{p}(x_1, y, t), \\ T(x_1, y, t) &= T(x_1, y) + \tilde{T}(x_1, y, t), \end{aligned} \quad (8)$$

where a quantity with a tilde is a perturbation quantity and is assumed to be small in comparison with the mean flow quantities. Equations 8 are substituted into Equations 1 to 5 and equations for mean quantities are used to subtract out the basic state. The resulting equations are linearized by neglecting all the terms which are nonlinear in perturbation quantities. The resulting mass, x -momentum, y -momentum, energy and state equations, respectively, are:

$$\frac{\partial \tilde{p}}{\partial t} + \varepsilon \frac{\partial}{\partial x_1} (R\tilde{u} + \tilde{\rho}U) + \frac{\partial}{\partial y} (R\tilde{v} + \tilde{\rho}V) = 0, \quad (9)$$

$$\begin{aligned} R \frac{\partial \tilde{u}}{\partial t} + \varepsilon R U \frac{\partial \tilde{u}}{\partial x_1} + \varepsilon R \frac{\partial U}{\partial x_1} \tilde{u} + \varepsilon U \frac{\partial U}{\partial x_1} \tilde{\rho} \\ + R \frac{\partial U}{\partial y} \tilde{v} + R V \frac{\partial \tilde{u}}{\partial y} + V \frac{\partial U}{\partial y} \tilde{\rho} \\ = \varepsilon \frac{\partial \tilde{p}}{\partial x_1} + \frac{1}{3\text{Re}} \left(4\varepsilon^2 \frac{\partial^2 \tilde{u}}{\partial x_1^2} - 2\varepsilon \frac{\partial^2 \tilde{u}}{\partial x_1 \partial y} \right. \\ \left. + \varepsilon \frac{\partial^2 v}{\partial x_1 \partial y} + 3 \frac{\partial^2 \tilde{u}}{\partial y^2} - 2 \frac{\partial^2 \tilde{v}}{\partial y^2} \right), \end{aligned} \quad (10)$$

$$\begin{aligned} R \frac{\partial \tilde{v}}{\partial t} + \varepsilon R U \frac{\partial \tilde{v}}{\partial x_1} + \varepsilon R \frac{\partial V}{\partial x_1} + \varepsilon U \frac{\partial V}{\partial x_1} \tilde{\rho} \\ + R V \frac{\partial \tilde{v}}{\partial y} + R \frac{\partial V}{\partial y} \tilde{v} + V \frac{\partial V}{\partial y} \tilde{\rho} \\ = \frac{\partial \tilde{p}}{\partial y} + \frac{1}{3\text{Re}} \left(-2\varepsilon^2 \frac{\partial^2 \tilde{u}}{\partial x_1^2} + 3\varepsilon^2 \frac{\partial^2 \tilde{v}}{\partial x_1^2} \right. \\ \left. + \varepsilon \frac{\partial^2 \tilde{u}}{\partial x_1 \partial y} - 2\varepsilon \frac{\partial^2 \tilde{v}}{\partial x_1 \partial y} + 4 \frac{\partial^2 \tilde{v}}{\partial y^2} \right), \end{aligned} \quad (11)$$

$$\begin{aligned} R \frac{\partial \tilde{T}}{\partial t} + \varepsilon R U \frac{\partial \tilde{T}}{\partial x_1} + \varepsilon R \frac{\partial T}{\partial x_1} \tilde{u} + \varepsilon U \frac{\partial T}{\partial x_1} \tilde{\rho} \\ + R V \frac{\partial \tilde{T}}{\partial y} + R \frac{\partial T}{\partial y} \tilde{v} + V \frac{\partial T}{\partial y} \tilde{\rho} \\ = (\gamma - 1) M^2 \left(\frac{\partial \tilde{p}}{\partial t} + \varepsilon U \frac{\partial \tilde{p}}{\partial x_1} + \varepsilon \frac{\partial P}{\partial x_1} \tilde{u} \right. \\ \left. + V \frac{\partial \tilde{p}}{\partial y} + \frac{\partial P}{\partial y} \tilde{v} \right) + \frac{(\gamma - 1) M^2}{\text{Re}} \left\{ 4\varepsilon^2 \frac{\partial U}{\partial x_1} \frac{\partial \tilde{u}}{\partial x_1} \right. \\ \left. + 4 \frac{\partial U}{\partial y} \frac{\partial \tilde{u}}{\partial y} + 2 \left(\frac{\partial \tilde{u}}{\partial y} + \varepsilon \frac{\partial \tilde{v}}{\partial x_1} \right) \cdot \left[\left(\frac{\partial U}{\partial y} + \varepsilon \frac{\partial V}{\partial x_1} \right) \right. \right. \\ \left. \left. \frac{1}{3} \left(\varepsilon \frac{\partial U}{\partial x_1} + \frac{\partial V}{\partial y} \right) \right] - \frac{2}{3} \left(\varepsilon \frac{\partial \tilde{u}}{\partial x_1} + \frac{\partial \tilde{v}}{\partial y} \right) \left[\varepsilon \frac{\partial V}{\partial x_1} \right. \right. \\ \left. \left. + \frac{\partial U}{\partial y} + 2 \left(\varepsilon \frac{\partial U}{\partial x_1} + \frac{\partial V}{\partial y} \right) \right] \right\}, \end{aligned} \quad (12)$$

$$\tilde{p} = \frac{1}{\gamma M^2} (R\tilde{T} + T\tilde{\rho}). \quad (13)$$

Equations 9 to 13 form a set of five equations for the five unknown perturbation quantities. Note that because of the non-parallelism effects of the mean flow, the

coefficients of the partial derivatives in these equations are functions of both independent variables, x_1 and y .

The boundary conditions in the x -direction are those of no slip and no penetration of the shear layer impinging at the trailing edge of the cavity. These are:

$$\tilde{u}(1, y) = 0, \quad \tilde{v}(1, y) = 0. \quad (14)$$

The boundary conditions in the y -direction are simply that the flow quantities must be bounded as $y \rightarrow \pm\infty$.

Governing Equations for Inviscid Shear Layer

For inviscid flow, the inverse of the Reynolds number approaches zero. The governing equations for a two-dimensional, inviscid, compressible shear layer are obtained by setting $1/\text{Re} = 0$ in system Equations 9 to 13.

Viscous Analysis of the Shear Layer

The viscous terms in the set of Equations 9 to 13 are important at the vicinity of the trailing edge of the cavity where the shear layer is impinging. This is like a typical boundary layer problem. The viscous terms are important near the wall and negligible anywhere away from the wall. Thus, the shear layer can be divided into two regions of inviscid (Outer region) and viscous (Inner region) flow, as in Figure 2. To retain the viscous terms, which were neglected in the outer region, the region in the vicinity of the wall is magnified by use of the following change of variables:

$$\xi = \frac{\varepsilon}{\varepsilon^\beta} x_1, \quad \beta > 1, \quad \eta = \frac{y}{\varepsilon^\alpha}, \quad \tau = \frac{t}{\varepsilon}, \quad (15)$$

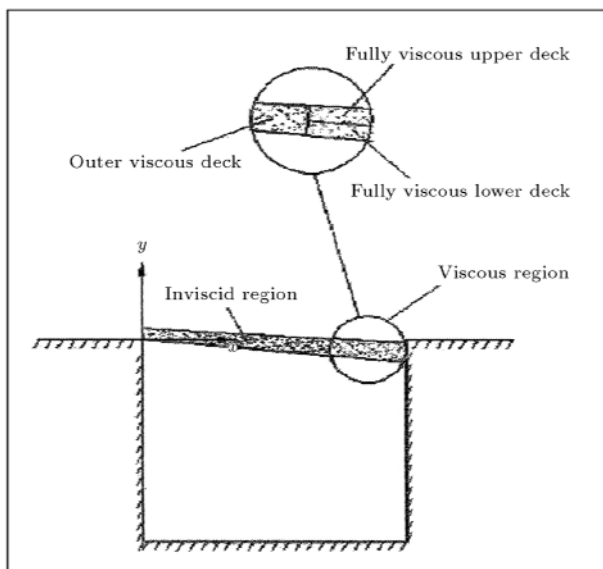


Figure 2. Triple-deck structure.

where the constants α and β are to be determined. The set of Equations 9 to 13 are written in new variables and the following expansions are used in these equations:

$$1/\text{Re} = \varepsilon/\text{Re}_1 + O(\varepsilon^2),$$

where:

$$1/\text{Re}_1 = O(1) \quad \text{and} \quad V = \varepsilon V_1 + O(\varepsilon^2). \quad (16)$$

The constants, α and β , are to be determined from balancing the order of magnitude of the terms contained in the set of these equations. Keeping the dominant terms by balancing each term in every equation with the rest of the terms, three sets of values for α and β yield a meaningful system of equations governing the viscous region, distinguished limits [28]. This is a multiple deck analysis, expected when inviscid and viscous regions interact in fluid mechanics problems. These distinct regions, shown in Figure 2 enclosed in a viscous region, are named as follows:

1. Fully viscous upper deck, when $\beta = 2, 0 \leq \alpha < 1$;
2. Fully viscous lower deck, in the case of $\beta = 2, \alpha = 1$;
3. Outer viscous deck, when $1 < \beta < 2, \alpha = 1$.

Substituting $\beta = 2, 0 \leq \alpha < 1$, into the system of Equations 9 to 13 in new variables gives the governing equations mass, momentum, energy and state for a fully viscous upper deck, respectively, as follows:

$$\frac{\partial \tilde{\rho}}{\partial \tau} - \frac{\partial (R\tilde{u} + U\tilde{\rho})}{\partial \xi} + \varepsilon^{(1-\alpha)} \frac{\partial (R\tilde{v} + V\tilde{\rho})}{\partial \eta} = 0, \quad (17)$$

$$\begin{aligned} & R \frac{\partial \tilde{u}}{\partial \tau} + R \frac{\partial U}{\partial \xi} \tilde{u} + RU \frac{\partial \tilde{u}}{\partial \xi} + U \frac{\partial U}{\partial \xi} \tilde{\rho} + \frac{4}{3\text{Re}_1} \frac{\partial^2 \tilde{u}}{\partial \xi^2} \\ & + \frac{\partial \tilde{p}}{\partial \xi} + \varepsilon^{(1-\alpha)} \left[\frac{1}{3\text{Re}_1} \left(2 \frac{\partial^2 \tilde{u}}{\partial \xi \partial \eta} - \frac{\partial^2 \tilde{v}}{\partial \xi \partial \eta} \right) \right. \\ & \left. R \frac{\partial U}{\partial \xi} \tilde{v} \right] + \varepsilon^{(2-2\alpha)} \left[\frac{1}{3\text{Re}_1} \left(3 \frac{\partial^2 \tilde{u}}{\partial \eta^2} - 2 \frac{\partial^2 \tilde{v}}{\partial \eta^2} \right) \right] \\ & \varepsilon^{(2-\alpha)} \left(V_1 \frac{\partial U}{\partial \eta} \tilde{\rho} + RV_1 \frac{\partial \tilde{u}}{\partial \eta} \right) \\ & = 0, \end{aligned} \quad (18)$$

$$\begin{aligned} & R \frac{\partial \tilde{v}}{\partial \tau} - \frac{1}{3\text{Re}_1} \left(2 \frac{\partial^2 \tilde{u}}{\partial \xi^2} - 3 \frac{\partial^2 \tilde{v}}{\partial \xi^2} \right) + U \frac{\partial V}{\partial \xi} \tilde{\rho} \\ & + R \frac{\partial V}{\partial \xi} \tilde{u} + RU \frac{\partial \tilde{v}}{\partial \xi} + \varepsilon^{(1-\alpha)} \left[\frac{1}{3\text{Re}_1} \left(2 \frac{\partial^2 \tilde{v}}{\partial \xi \partial \eta} \right) \right. \end{aligned}$$

$$\begin{aligned} & \left. \frac{\partial^2 \tilde{u}}{\partial \xi \partial \eta} \right) R \frac{\partial V}{\partial \eta} \tilde{v} \left. \frac{\partial \tilde{p}}{\partial \eta} \right] + \varepsilon^{(2-2\alpha)} \left(\frac{4}{3\text{Re}_1} \frac{\partial^2 \tilde{v}}{\partial \eta^2} \right) \\ & \varepsilon^{(2-\alpha)} \left(V_1 \frac{\partial V}{\partial \eta} \tilde{\rho} + R V_1 \frac{\partial \tilde{v}}{\partial \eta} \right) \\ = 0, \end{aligned} \quad (19)$$

$$\begin{aligned} & R \frac{\partial T}{\partial \tau} \tilde{u} \quad R U \frac{\partial T}{\partial \xi} \tilde{u} \quad R \frac{\partial T}{\partial \xi} \tilde{u} \quad U \frac{\partial T}{\partial \xi} \tilde{\rho} \quad (\gamma-1) M^2 \left(\frac{\partial \tilde{p}}{\partial \tau} \right. \\ & \left. U \frac{\partial \tilde{p}}{\partial \xi} \quad \frac{\partial p}{\partial \xi} \tilde{u} \right) \frac{2(\gamma-1) M^2}{3\text{Re}_1} \left(6 \frac{\partial U}{\partial \xi} \frac{\partial \tilde{u}}{\partial \xi} + 3 \frac{\partial V}{\partial \xi} \frac{\partial \tilde{v}}{\partial \xi} \right. \\ & \left. \frac{\partial U}{\partial \xi} \frac{\partial \tilde{v}}{\partial \xi} \quad \frac{\partial V}{\partial \xi} \frac{\partial \tilde{u}}{\partial \xi} \quad 2 \frac{\partial U}{\partial \xi} \frac{\partial \tilde{u}}{\partial \xi} \right) + \varepsilon^{(1-\alpha)} \left[R V \frac{\partial T}{\partial \eta} \right. \\ & \left. + R \frac{\partial T}{\partial \eta} \tilde{v} + V \frac{\partial T}{\partial \eta} \tilde{\rho} \quad (\gamma-1) M^2 \left(V \frac{\partial \tilde{p}}{\partial \eta} + \frac{\partial p}{\partial \eta} \tilde{v} \right) \right. \\ & \left. \frac{2(\gamma-1) M^2}{3\text{Re}_1} \left(3 \frac{\partial V}{\partial \xi} \frac{\partial \tilde{u}}{\partial \eta} + \frac{\partial U}{\partial \xi} \frac{\partial \tilde{u}}{\partial \eta} \quad 3 \frac{\partial U}{\partial \eta} \frac{\partial \tilde{v}}{\partial \xi} \right. \right. \\ & \left. \left. + \frac{\partial V}{\partial \eta} \frac{\partial \tilde{v}}{\partial \xi} + \frac{\partial U}{\partial \eta} \frac{\partial \tilde{u}}{\partial \xi} + 2 \frac{\partial V}{\partial \eta} \frac{\partial \tilde{u}}{\partial \xi} + \frac{\partial V}{\partial \xi} \frac{\partial \tilde{v}}{\partial \eta} \right. \right. \\ & \left. \left. + 2 \frac{\partial U}{\partial \xi} \frac{\partial \tilde{v}}{\partial \eta} \right] \quad \varepsilon^{(2-2\alpha)} \frac{2(\gamma-1) M^2}{3\text{Re}_1} \left(9 \frac{\partial U}{\partial \eta} \frac{\partial \tilde{u}}{\partial \eta} \right. \right. \\ & \left. \left. \frac{\partial V}{\partial \eta} \frac{\partial \tilde{u}}{\partial \eta} \quad \frac{\partial U}{\partial \eta} \frac{\partial \tilde{v}}{\partial \eta} \quad 2 \frac{\partial V}{\partial \eta} \frac{\partial \tilde{v}}{\partial \eta} \right) \right) \\ = 0, \end{aligned} \quad (20)$$

$$\tilde{p} = \frac{1}{\gamma M^2} (R \tilde{T} + T \tilde{\rho}). \quad (21)$$

For any value of $0 \leq \alpha < 1$, the first order terms in the set of equations above are the coefficients of $\varepsilon^{(1-\alpha)}$. The choice of perturbation parameter in this deck is $\varepsilon_2 = \varepsilon^{(1-\alpha)}$. The solution to this system is to be matched asymptotically to the solutions resulting from the system equations 1) Fully viscous lower deck and 2) Outer viscous deck, respectively. In the process of this matching, the proper value of α is determined.

Substituting $\beta = 2$ and $\alpha = 1$ into system Equations 9 to 13 in new variables gives the governing equations mass, momentum, energy and state for a fully viscous lower deck. The solution to this system is to be matched asymptotically to the solution resulting from the system equations governing 1) Fully

viscous upper deck and 2) Outer viscous deck, respectively.

Substituting $1 < \beta < 2$ and $\alpha = 1$ into system Equations 9 to 13 in new variables gives the governing equations mass, momentum, energy and state for the outer viscous deck, respectively, as:

$$\frac{\partial \tilde{\rho}}{\partial \tau} \quad \varepsilon^{(2-\beta)} \frac{\partial}{\partial \xi} (R \tilde{u} + U \tilde{\rho}) + \frac{\partial}{\partial \eta} (R \tilde{v} + V \tilde{\rho}) = 0, \quad (22)$$

$$\begin{aligned} & R \frac{\partial \tilde{u}}{\partial \tau} + \frac{1}{3\text{Re}_1} \left(3 \frac{\partial^2 \tilde{u}}{\partial \eta^2} \quad 2 \frac{\partial^2 \tilde{v}}{\partial \eta^2} \right) \quad R \frac{\partial U}{\partial \eta} \tilde{v} \\ & + \varepsilon^{(2-\beta)} \left[\frac{1}{3\text{Re}_1} \left(2 \frac{\partial^2 \tilde{u}}{\partial \xi \partial \eta} \quad \frac{\partial^2 \tilde{v}}{\partial \xi \partial \eta} \right) + U \frac{\partial U}{\partial \xi} \tilde{\rho} \right. \\ & \left. + R U \frac{\partial \tilde{u}}{\partial \xi} + R \frac{\partial U}{\partial \xi} \tilde{u} + \frac{\partial \tilde{p}}{\partial \xi} \right] + \varepsilon^{(4-2\beta)} \frac{4}{3\text{Re}_1} \frac{\partial^2 \tilde{u}}{\partial \xi^2} \\ & \quad \varepsilon (V_1 \frac{\partial U}{\partial \eta} \tilde{\rho} + R V_1 \frac{\partial \tilde{u}}{\partial \eta}) \\ = 0, \end{aligned} \quad (23)$$

$$\begin{aligned} & R \frac{\partial \tilde{v}}{\partial \tau} + \frac{4}{3\text{Re}_1} \frac{\partial^2 \tilde{v}}{\partial \eta^2} \quad R \frac{\partial V}{\partial \eta} \tilde{v} \quad \frac{\partial \tilde{p}}{\partial \eta} \\ & + \varepsilon^{(2-\beta)} \left[\frac{1}{3\text{Re}_1} \left(2 \frac{\partial^2 \tilde{v}}{\partial \xi \partial \eta} \quad \frac{\partial^2 \tilde{u}}{\partial \xi \partial \eta} \right) + U \frac{\partial V}{\partial \xi} \tilde{\rho} \right. \\ & \left. + R \frac{\partial V}{\partial \xi} \tilde{u} + R U \frac{\partial \tilde{v}}{\partial \xi} \right] + \varepsilon^{(4-2\beta)} \frac{1}{3\text{Re}_1} \left(2 \frac{\partial^2 \tilde{u}}{\partial \xi^2} \right. \\ & \left. + 3 \frac{\partial^2 \tilde{v}}{\partial \xi^2} \right) \quad \varepsilon \left(V_1 \frac{\partial V}{\partial \eta} \tilde{\rho} + R V_1 \frac{\partial \tilde{v}}{\partial \eta} \right) = 0, \end{aligned} \quad (24)$$

$$\begin{aligned} & R \frac{\partial T}{\partial \tau} \tilde{u} + R V \frac{\partial T}{\partial \eta} \tilde{u} + R \frac{\partial T}{\partial \eta} \tilde{v} + V \frac{\partial T}{\partial \eta} \tilde{\rho} \quad (\gamma-1) M^2 \left(\frac{\partial \tilde{p}}{\partial \tau} \right. \\ & \left. + V \frac{\partial \tilde{p}}{\partial \eta} + \frac{\partial P}{\partial \eta} \tilde{v} \right) \frac{2(\gamma-1) M^2}{3\text{Re}_1} \left(9 \frac{\partial U}{\partial \eta} \frac{\partial \tilde{u}}{\partial \eta} \right. \\ & \left. \frac{\partial V}{\partial \eta} \frac{\partial \tilde{u}}{\partial \eta} \quad \frac{\partial U}{\partial \eta} \frac{\partial \tilde{v}}{\partial \eta} \quad 2 \frac{\partial V}{\partial \eta} \frac{\partial \tilde{v}}{\partial \eta} \right) + \varepsilon^{(2-\beta)} \left[R U \frac{\partial T}{\partial \xi} \right. \\ & \left. R \frac{\partial T}{\partial \xi} \tilde{u} \quad U \frac{\partial T}{\partial \xi} \tilde{\rho} + (\gamma-1) M^2 \left(U \frac{\partial \tilde{p}}{\partial \xi} + \frac{\partial P}{\partial \xi} \tilde{u} \right) \right. \\ & \left. \frac{2(\gamma-1) M^2}{3\text{Re}_1} \left(3 \frac{\partial V}{\partial \xi} \frac{\partial \tilde{u}}{\partial \eta} \quad 3 \frac{\partial U}{\partial \eta} \frac{\partial \tilde{v}}{\partial \xi} + \frac{\partial U}{\partial \xi} \frac{\partial \tilde{u}}{\partial \eta} \right) \right) \end{aligned}$$

$$\begin{aligned}
& + \frac{\partial V}{\partial \eta} \frac{\partial \tilde{v}}{\partial \xi} + \frac{\partial U}{\partial \eta} \frac{\partial \tilde{u}}{\partial \xi} + \frac{\partial V}{\partial \xi} \frac{\partial \tilde{v}}{\partial \eta} + 2 \frac{\partial V}{\partial \eta} \frac{\partial \tilde{u}}{\partial \eta} \\
& + 2 \left[\frac{\partial U}{\partial \xi} \frac{\partial \tilde{v}}{\partial \eta} \right] \varepsilon^{(4-2\beta)} \frac{2(\gamma-1)M^2}{3\text{Re}_1} \left(6 \frac{\partial U}{\partial \xi} \frac{\partial \tilde{u}}{\partial \xi} \right. \\
& \left. + 3 \frac{\partial V}{\partial \xi} \frac{\partial \tilde{v}}{\partial \xi} - \frac{\partial U}{\partial \xi} \frac{\partial \tilde{v}}{\partial \xi} - \frac{\partial V}{\partial \xi} \frac{\partial \tilde{u}}{\partial \xi} - 2 \frac{\partial U}{\partial \xi} \frac{\partial \tilde{u}}{\partial \xi} \right) \\
& = 0, \tag{25}
\end{aligned}$$

$$\tilde{p} = \frac{1}{\gamma M^2} (R\tilde{T} + T\tilde{\rho}). \tag{26}$$

For any value of $1 < \beta < 2$, the first order terms in the set of these equations are the coefficients of $\varepsilon^{(2-\beta)}$. The choice of perturbation parameter in this deck is $\varepsilon_1 = \varepsilon^{(2-\beta)}$. The solution to this system is to be matched asymptotically to the solutions resulting from the system equations governing the 1) Outer viscous deck and 2) Fully viscous upper and lower decks, respectively. In the process of this matching, the proper value of β is determined. This section completes the formulation of the problem of a two-dimensional compressible, viscous shear layer spanning an open cavity. In the next section, the normal mode analysis is presented.

NORMAL MODE ANALYSIS

In this section, the stability characteristics of the shear layer are considered when it is excited by a reflected wave of frequency ω . Since the mean flow is non-parallel and its properties are functions of both spatial variables, x and y or ξ and η in the viscous regions, the standard parallel stability theory is not appropriate in this problem. Here, the amplitude functions are assumed functions of both coordinates x and y or ξ and η and a perturbation method (multiple scales), in conjunction with normal mode theory, is used.

For inviscid shear layer, it is convenient to expand the mean flow quantities, according to expansions (Equations 16) in the power series in ε , as:

$$Q(x_1, y) = Q_o(x_1, y) + \varepsilon Q_1(x_1, y) + \dots, \tag{27}$$

in which Q represents U, V, R, P, T . Additionally, the perturbation quantities will be decomposed into an amplitude, which is a function of two variables times an exponential function, whose exponent is also a function of two variables. To this end, let:

$$\tilde{u}(x_1, y, t) = a(x_1, y) e^{i\theta(x_1, t)},$$

$$\tilde{v}(x_1, y, t) = b(x_1, y) e^{i\theta(x_1, t)},$$

$$\tilde{\rho}(x_1, y, t) = c(x_1, y) e^{i\theta(x_1, t)},$$

$$\tilde{p}(x_1, y, t) = d(x_1, y) e^{i\theta(x_1, t)},$$

$$\tilde{T}(x_1, y, t) = f(x_1, y) e^{i\theta(x_1, t)}, \tag{28}$$

where:

$$\partial\theta/\partial t = \omega \text{ is frequency and } \partial\theta/\partial x_1 = k(x_1). \tag{29}$$

It is noted that both the amplitudes and the wave number, k , are assumed to be functions of the slow scale, x_1 , as opposed to the standard linear stability problem, where k is constant and the amplitudes are only functions of the y -coordinate [30]. It is also convenient to expand the amplitude functions in the power series of ε . Thus;

$$\text{amp}(x_1, y) = \text{amp}_o(x_1, y) + \varepsilon \text{amp}_1(x_1, y) + \dots,$$

$$k(x_1) = \frac{1}{\varepsilon} k(x_1) + \dots \tag{30}$$

in which amp represents a, b, c, d and f .

Equations 30 are substituted into Equations 28. The resulting equations are substituted into governing equations for inviscid shear layer, making use of Equation 27. Coefficients of like powers of ε are collected in each equation and set equal to zero independently. The results are summarized below:

Order ε^0 :

Mass, x -momentum, y -momentum, energy and state are, respectively, as follows:

$$i k R_o a_o + R_o \frac{\partial b_o}{\partial y} + \frac{\partial R_o}{\partial y} b_o + i(k U_o - \omega) c_o = 0, \tag{31}$$

$$i(k U_o - \omega) R_o a_o + R_o \frac{\partial U_o}{\partial y} b_o + i k d_o = 0, \tag{32}$$

$$i(k U_o - \omega) R_o b_o + \frac{\partial d_o}{\partial y} = 0, \tag{33}$$

$$\begin{aligned}
& \left[R_o \frac{\partial T_o}{\partial y} - (\gamma - 1) M^2 \frac{\partial p_o}{\partial y} \right] b_o \\
& - (\gamma - 1) M^2 i (k U_o - \omega) d_o \\
& + i(k U_o - \omega) R_o f_o \\
& = 0, \tag{34}
\end{aligned}$$

$$\frac{1}{\gamma M^2} T_o c_o - d_o + \frac{1}{\gamma M^2} R_o f_o = 0. \tag{35}$$

Order ε :

Mass, x -momentum, y -momentum, energy and state are, respectively, as follows:

$$\begin{aligned}
& ikR_o a_1 + R_o \frac{\partial b_1}{\partial y} + \frac{\partial R_o}{\partial y} b_1 + i(kU_o - \omega)c_1 = \\
& R_o \frac{\partial a_o}{\partial x_1} - a_o \frac{\partial R_o}{\partial x_1} - U_o \frac{\partial c_o}{\partial x_1} - c_o \frac{\partial U_o}{\partial x_1} \\
& ikR_1 a_o - ikU_1 c_o - R_1 \frac{\partial b_o}{\partial y} - b_o \frac{\partial R_1}{\partial y} \\
& V_1 \frac{\partial c_o}{\partial y} - c_o \frac{\partial V_1}{\partial y}, \quad (36)
\end{aligned}$$

$$\begin{aligned}
& i(kU_o - \omega)R_o a_1 + R_o \frac{\partial U_o}{\partial y} b_1 + ikd_1 \\
& = R_o U_o \frac{\partial a_o}{\partial x_1} - R_o a_o \frac{\partial U_o}{\partial x_1} - c_o U_o \frac{\partial U_o}{\partial x_1} - \frac{\partial d_o}{\partial x_1} \\
& + i(kU_o - \omega)a_o R_1 - ikU_1 a_o R_o - V_1 R_o \frac{\partial a_o}{\partial y} \\
& R_o b_o \frac{\partial U_1}{\partial y} - R_1 b_o \frac{\partial U_o}{\partial y} - V_1 c_o \frac{\partial U_o}{\partial y}, \quad (37)
\end{aligned}$$

$$\begin{aligned}
& i(kU_o - \omega)R_o b_1 + \frac{\partial d_1}{\partial y} \\
& = i(kU_o - \omega)b_o R_1 - R_o U_o \frac{\partial b_o}{\partial x_1} \\
& ikR_o b_o U_1 - V_1 R_o \frac{\partial b_o}{\partial y} - R_o b_o \frac{\partial V_1}{\partial y}, \quad (38)
\end{aligned}$$

$$\begin{aligned}
& \left[R_o \frac{\partial T_o}{\partial y} - (\gamma - 1)M^2 \frac{\partial p_o}{\partial y} \right] b_1 \\
& (\gamma - 1)M^2 i(kU_o - \omega)d_1 + i(kU_o - \omega)R_o f_1 \\
& = i(kU_o - \omega)R_1 f_o + R_o U_o \frac{\partial f_o}{\partial x_1} \\
& ikR_o U_1 f_o - R_o a_o \frac{\partial T_o}{\partial x_1} - V_1 R_o \frac{\partial f_o}{\partial y} \\
& R_o b_o \frac{\partial T_1}{\partial y} - R_1 b_o \frac{\partial T_o}{\partial y} - U_o c_o \frac{\partial T_o}{\partial x_1} \\
& V_1 c_o \frac{\partial T_o}{\partial y} + (\gamma - 1)M^2 \left[U_o \frac{\partial d_o}{\partial x_1} + ikU_1 d_o \right. \\
& \left. + a_o \frac{\partial p_o}{\partial x_1} + V_1 \frac{\partial d_o}{\partial y} + b_o \frac{\partial p_1}{\partial y} \right], \quad (39)
\end{aligned}$$

$$\begin{aligned}
& \frac{1}{\gamma M^2} T_o c_1 - d_1 + \frac{1}{\gamma M^2} R_o f_1 = \\
& \frac{1}{\gamma M^2} (R_1 f_o + T_1 c_o). \quad (40)
\end{aligned}$$

Equations 31 to 35 represent a set of equations to be solved for the zeroth order perturbation amplitudes a_o , b_o , c_o , d_o and f_o . This will be presented in later sections.

For viscous shear layer, in the same way, the mean flow properties and amplitudes are expanded in the power series in ε as before, but, in terms of ξ and η and different ones in each deck. Zeroth-order and first-order mass, x -momentum, y -momentum, energy and state equations, in a form similar to Equations 31 through 40 for perturbation amplitudes, are obtained for each deck in the multiple deck structure. These equations are to be solved for each deck independently and then the results are to be matched asymptotically to those among themselves, as well as to the inviscid region. This task will be presented in the next sections.

DERIVATION OF WAVE-NUMBER CORRECTION

The wave-number correction, due to the effect of the non-parallelism of the shear layer, is derived in this section. This is done for the inviscid region, as well as for the amplitude deck structure in the viscous region. The system of equations for zeroth and first-order amplitudes in every region is written in a matrix form involving a linear operator. The adjoint of this operator is calculated and the Fredholm alternative is applied. The resulting solvability condition produces a differential equation yielding to the derivation of the wave-number/frequency correction. This correction is added to the wave-number/frequency calculated by Tam and Block. The corrected wave-number is matched throughout the region asymptotically.

Wave-Number Correction for Inviscid Region

System Equations 31 to 35 represent a set of equations to be solved for the zeroth-order perturbation amplitudes a_o , b_o , c_o , d_o and f_o for the inviscid region. This set of equations can be written in matrix form as:

$$[L][\phi_o(x_1, y)] = [0], \quad (41)$$

where:

$$[\phi_o] = [a_o \quad b_o \quad c_o \quad d_o \quad f_o]^T,$$

and:

$$[L] = \begin{bmatrix} ikR_o & \frac{\partial R_o}{\partial y} + R_o \frac{\partial}{\partial y} & i(kU_o - \omega) \\ i(kU_o - \omega)R_o & R_o \frac{\partial U_o}{\partial y} & 0 \\ 0 & i(kU_o - \omega)R_o & 0 \\ 0 & R_o \frac{\partial T_o}{\partial y} & 0 \\ 0 & 0 & \frac{T_o}{\gamma M^2} \\ 0 & 0 & 0 \\ ik & 0 & 0 \\ \frac{\partial}{\partial y} & 0 & 0 \\ i(\gamma - 1)M^2(kU_o - \omega) & i(kU_o - \omega)R_o & 0 \\ 1 & \frac{R_o}{\gamma M^2} & 0 \end{bmatrix}. \quad (42)$$

It is noted that the operations involved in $[L]$ are simply multiplications by known functions and differentiations with respect to y . Thus, it is possible to consider Equation 41 at a given spanwise location independent of every other spanwise location. This is a result of the weakly non-parallel approximation. Arbitrary functions of x_1 will be involved in the solution of Equation 41. Indeed, it is convenient to write:

$$[\phi_o(x_1, y)] = A(x_1)[\hat{\phi}_o(x_1, y)], \quad (43)$$

where $A(x_1)$ is, at this level, an arbitrary function of x . However, since differentiations in $[L]$ are with respect to y only:

$$[L][\phi_o(x_1, y)] = A(x_1)[L][\hat{\phi}_o(x_1, y)],$$

or:

$$[L][\hat{\phi}_o(x_1, y)] = [0]. \quad (44)$$

Equation 44 is a homogeneous system of equations to solve for the components of $[\phi_o(x_1, y)]$. The matrix, $[L]$, is a matrix of linear operators that acts on the components of a five-dimensional vector which are functions of y and transforms it into a new five-dimensional vector. Thus, the vector space, \mathfrak{R} , is defined as all five-dimensional vectors whose components are complex functions of a real variable, y , whose range is from $-\infty$ to $+\infty$. An inner product can be defined on this vector space according to:

$$([r], [s]) = \int_{-\infty}^{+\infty} [r]^T [\bar{s}] dy, \quad (45)$$

for all $[r], [s] \in \mathfrak{R}$. The bar in Equation 45 denotes a complex conjugate. For a given excitation frequency, ω , it is desired to find the amplitudes of each variable, as well as the spatial wave function, $k(x_1)$. Equation 44 is a homogeneous system for solving these amplitudes at

each spatial location with the local value of $k(x_1)$ as a parameter. However, this system will have a non-trivial solution only for certain values of $k(x_1)$. The values of $k(x_1)$, for which this non-trivial solution occurs, can be determined numerically. Equations 36 to 40 represent a set of equations to solve for the first-order perturbation amplitudes a_1, b_1, c_1, d_1 and f_1 . These equations can be written in the form:

$$[L][\phi_1(x_1, y)] = [g(x_1, y)], \quad (46)$$

where:

$$[\phi_1(x_1, y)] = [a_1 \ b_1 \ c_1 \ d_1 \ f_1]^T,$$

$$[g(x_1, y)] = [g_1(x_1, y) \ g_2(x_2, y) \ g_3(x_1, y) \ g_4(x_1, y) \ g_5(x_1, y)]^T,$$

in which g 's are the right hand-side functions of Equations 36 to 40, respectively. The operator, $[L]$, in Equation 44 is the same operator that appears in Equation 46. This equation is a non-homogeneous system, whereas Equation 44 is a homogeneous system. Furthermore, non-trivial solutions of Equation 46 exist. Thus, the Fredholm alternative implies that a solution to Equation 46 exists if, and only if, the non-homogeneous terms satisfy a solvability condition. In particular, one can show that the non-homogeneous terms must be orthogonal to all non-trivial solutions of the corresponding adjoint problem. The adjoint of an operator, $[L]$, with respect to a given inner product, is the operator, $[L^*]$, that:

$$([L][r], [s]) = ([r], [L^*][s]), \quad (47)$$

for all $[r], [s]$ belonging to the domain of $[L]$. Equation 47 applied to the inner product given in Equation 45 becomes:

$$\int_{-\infty}^{+\infty} ([L][r])^T [\bar{s}] dy = \int_{-\infty}^{+\infty} [r]^T ([L^*][\bar{s}]) dy. \quad (48)$$

Let, $[r] = [r_1 \ r_2 \ r_3 \ r_4 \ r_5]^T$ and $[s] = [s_1 \ s_2 \ s_3 \ s_4 \ s_5]^T$ be arbitrary elements of \mathfrak{R} . Then, using the definition of $[L]$ from Equation 44, the left-hand side of Equation 48 becomes:

$$\int_{-\infty}^{+\infty} ([L][r])^T [\bar{s}] dy = \int_{-\infty}^{+\infty} \left\{ \left[ikR_o r_1 + \frac{\partial R_o}{\partial y} r_2 + R_o \frac{\partial r_2}{\partial y} + i(kU_o - \omega)r_3 \right] \bar{s}_1 + \left[i(kU_o - \omega)R_o r_1 + R_o \frac{\partial U_o}{\partial y} r_2 \right] \bar{s}_2 \right\} dy$$

$$\begin{aligned}
& + ikr_4 \bar{s}_2 + \left[i(kU_o - \omega)R_o r_2 + \frac{\partial r_4}{\partial y} \right] \bar{s}_3 + \left[R_o \frac{\partial T_o}{\partial y} r_2 \right. \\
& \quad \left. i(\gamma - 1)M^2(kU_o - \omega)r_4 + i(kU_o - \omega)R_o r_5 \right] \bar{s}_4 \\
& + \left[\frac{T_o}{\gamma M^2} r_3 + r_4 - \frac{R_o}{\gamma M^2} r_5 \right] \bar{s}_5 \Big\} dy.
\end{aligned}$$

By use of integration by parts, this can be written as:

$$\begin{aligned}
\int_{-\infty}^{+\infty} ([L][r])^T [\bar{s}] dy &= \int_{-\infty}^{+\infty} \left\{ \left[ikR_o \bar{s}_1 + i(kU_o - \omega)R_o \bar{s}_2 \right] r_1 \right. \\
& + \left[\frac{\partial R_o}{\partial y} \bar{s}_1 - \frac{\partial}{\partial y} (R_o \bar{s}_1) + R_o \frac{\partial U_o}{\partial y} \bar{s}_2 + i(kU_o - \omega)R_o \bar{s}_3 \right. \\
& + R_o \frac{\partial T_o}{\partial y} \bar{s}_4 \Big] r_2 + \left[i(kU_o - \omega) \bar{s}_1 - \frac{T_o}{\gamma M^2} \bar{s}_5 \right] r_3 \\
& + \left[ik \bar{s}_2 - i(\gamma - 1)M^2(kU_o - \omega) \bar{s}_4 + \bar{s}_5 - \frac{\partial \bar{s}_3}{\partial y} \right] r_4 \\
& \left. + \left[i(kU_o - \omega)R_o \bar{s}_4 - \frac{R_o}{\gamma M^2} \bar{s}_5 \right] r_5 \right\} dy. \quad (49)
\end{aligned}$$

The right-hand side of Equation 49 can be written in the same form as the right-hand side of Equation 48 with:

$$\begin{aligned}
[L^*] &= \\
& \left\{ \begin{array}{ccc} i\bar{k}R_o & i(\bar{k}U_o - \omega)R_o & 0 \\ R_o \frac{\partial}{\partial y} & R_o \frac{\partial U_o}{\partial y} & i(\bar{k}U_o - \omega)R_o \\ i(\bar{k}U_o - \omega) & 0 & 0 \\ 0 & i\bar{k} & \frac{\partial}{\partial y} \\ 0 & 0 & 0 \end{array} \right. \\
& \left. \begin{array}{ccc} 0 & 0 \\ R_o \frac{\partial T_o}{\partial y} & 0 \\ 0 & \frac{T_o}{\gamma M^2} \\ i(\gamma - 1)M^2(\bar{k}U_o - \omega) & 1 \\ i(\bar{k}U_o - \omega) & \frac{R_o}{\gamma M^2} \end{array} \right\}.
\end{aligned}$$

Let $[\hat{\phi}_o^*(x_1, y)]$ be the solution to:

$$[L^*][\hat{\phi}_o^*(x_1, y)] = [0], \quad (50)$$

subject to the requirement that all components of $[\hat{\phi}_o^*(x_1, y)]$ are bounded as $y \rightarrow \pm\infty$. The Fredholm alternative implies that for a solution of Equation 44 to exist, $[g(x_1, y)]$ must be orthogonal to $[\hat{\phi}_o^*(x_1, y)]$. That is:

$$([g(x_1, y)], [\hat{\phi}_o^*(x_1, y)]) = 0,$$

or:

$$\int_{-\infty}^{+\infty} [g(x_1, y)]^T [\hat{\phi}_o^*(x_1, y)] dy = 0. \quad (51)$$

Upon substitution of all appropriate quantities and neglecting first-order perturbation quantities, Equation 51 becomes:

$$\begin{aligned}
A(x_1) \int_{-\infty}^{+\infty} \left\{ \left[R_o \frac{\partial \hat{a}_o}{\partial x_1} + \frac{\partial R_o}{\partial x_1} \hat{a}_o + U_o \frac{\partial \hat{c}_o}{\partial x_1} + \frac{\partial U_o}{\partial x_1} \hat{c}_o \right] \hat{a}_o^* \right. \\
+ \left[R_o U_o \frac{\partial \hat{a}_o}{\partial x_1} + R_o \frac{\partial U_o}{\partial x_1} \hat{a}_o + U_o \frac{\partial U_o}{\partial x_1} \hat{c}_o + \frac{\partial \hat{d}_o}{\partial x_1} \right] \hat{b}_o^* \\
+ \left[R_o U_o \frac{\partial \hat{b}_o}{\partial x_1} \right] \hat{c}_o^* + \left[R_o U_o \frac{\partial \hat{f}_o}{\partial x_1} + R_o \frac{\partial T_o}{\partial x_1} \hat{a}_o \right. \\
+ U_o \frac{\partial T_o}{\partial x_1} \hat{c}_o - (\gamma - 1)M^2 U_o \frac{\partial \hat{d}_o}{\partial x_1} \Big] \hat{d}_o^* \Big\} dy \\
+ \frac{dA}{dx_1} \int_{-\infty}^{+\infty} \left\{ (R_o \hat{a}_o + U_o \hat{c}_o) \hat{a}_o^* + (R_o U_o \hat{a}_o + \hat{d}_o) \hat{b}_o^* \right. \\
+ R_o U_o \hat{b}_o \hat{c}_o^* + \left[R_o U_o \hat{f}_o - (\gamma - 1)M^2 U_o \hat{d}_o \right] \hat{d}_o^* \Big\} dy = 0, \quad (52)
\end{aligned}$$

or:

$$\mu_1(x_1) \frac{dA}{dx_1} - i\mu_2(x_1)A(x_1) = 0, \quad (53)$$

where $\mu_1(x_1)$ and $\mu_2(x_1)$ can be determined by comparing Equations 52 to 53. The solution of Equation 53 is:

$$A(x_1) = A_o e^{+i \int \frac{\mu_2(x_1)}{\mu_1(x_1)} dx_1} = A_o e^{+i\nu(x_1)}, \quad (54)$$

where A_o is an arbitrary constant of integration. The solution for the zeroth-order perturbation quantities can be written as:

$$\tilde{u}(x_1, y) = A_o e^{i[k(x_1) + \nu(x_1) - \omega t]} a_o(x_1, y) + \dots,$$

$$\tilde{v}(x_1, y) = A_o e^{i[k(x_1) + \nu(x_1) - \omega t]} b_o(x_1, y) + \dots,$$

$$\tilde{\rho}(x_1, y) = A_o e^{i[k(x_1) + \nu(x_1) - \omega t]} c_o(x_1, y) + \dots,$$

$$\tilde{p}(x_1, y) = A_o e^{i[k(x_1) + \nu(x_1) - \omega t]} d_o(x_1, y) + \dots,$$

$$\tilde{T}(x_1, y) = A_o e^{i[k(x_1) + \nu(x_1) - \omega t]} f_o(x_1, y) + \dots$$

The sum:

$$\lambda(x_1) = k(x_1) + \nu(x_1), \quad (55)$$

represents a corrected value for the wave-number to include the effects of the shear layer thickness increasing downstream. The value of $\lambda(L)$ is dependent upon the frequency at which the shear layer is excited. A numerically defined function, $\lambda(L)$, for a given ω is defined. This function can then be used as a correction to the $k(\omega)$ used by Tam and Block.

Wave-Number Correction for Viscous Region

In such a manner as the previous section, the wave-number/frequency correction for the viscous region is derived. Here, in the same way, the mean flow properties and amplitudes are expanded in the power series in ε as follows, each deck with different ξ and η coordinates:

$$Q(\xi, \eta) = Q_o(\xi, \eta) + \varepsilon Q_1(\xi, \eta) + \dots,$$

and introducing normal modes as in Equations 28, but, in terms of ξ , η and τ , where $\frac{\partial \theta}{\partial \tau} = \omega$ and $\frac{\partial \theta}{\partial \xi} = k(\xi)$. Also, in the same way as in Equations 30, the amplitudes are expanded, but, in terms of ξ and η . Substituting these expansions in governing equations in the viscous region (Equations 17 to 21 for a fully viscous upper deck, Equations 17 to 21 with $\alpha = 1$ for a fully viscous lower deck and Equations 22 to 26 for the outer viscous deck), the systems equations for perturbation amplitudes in multiple deck structures are obtained. The wave-number correction for this region is derived in such a manner as the previous section.

NUMERICAL SOLUTION OF SHEAR LAYER EQUATIONS

In this section, the solution of the zeroth-order perturbation amplitudes for the inviscid region, as well as for the multiple deck structure, is presented. These zeroth-order perturbation amplitudes are used in the derived functions for the wave-number/frequency corrections due to the effect of non-parallelism of the shear layer, given in the previous section. An elimination process is used to reduce the system of equations representing the zeroth-order perturbation amplitudes to a differential equation of second order or to a system of differential equations of second order. The fourth order Runge-Kutta is used to solve these resulting differential equations numerically. All mean flow quantities are assumed to be known. In fact, a tangent hyperbolic function is assumed to represent the mean flow velocity profiles as follows:

$$U_o = \frac{1}{2} \left[1 + \tanh \left(\frac{y/L}{2\theta_o/L(1 + \beta x)} \right) \right]. \quad (56)$$

Here, all the quantities are dimensionless, θ_o is the thickness of the shear layer and β represents the rate of growth of the shear layer. Other mean flow properties, such as density, temperature and free stream speed of sound, are:

$$R_o = \frac{1}{1 + \frac{\gamma-1}{2} M^2 (1 - U_o^2)},$$

$$T_o = 1/R_o, \quad A_o = \frac{1}{M} \sqrt{1/R_o}. \quad (57)$$

By the use of these mean flow properties and a given frequency, ω , the zeroth-order amplitudes are solved and are used in evaluating the correction functions, $\nu(x_1)$. First, the numerical solution for zeroth-order amplitudes in the inviscid region is considered. The component equations of Equation 44 are:

$$ikR_o \hat{a}_o + R_o \frac{\partial \hat{b}_o}{\partial y} + \frac{\partial R_o}{\partial y} \hat{b}_o + i(kU_o - \omega) \hat{c}_o = 0, \quad (58)$$

$$i(kU_o - \omega) R_o \hat{a}_o + R_o \frac{\partial U_o}{\partial y} \hat{b}_o + ik \hat{d}_o = 0, \quad (59)$$

$$i(kU_o - \omega) R_o \hat{b}_o + \frac{\partial \hat{d}_o}{\partial y} = 0, \quad (60)$$

$$\left[R_o \frac{\partial T_o}{\partial y} - (\gamma - 1) M^2 \frac{\partial p_o}{\partial y} \right] \hat{b}_o - (\gamma - 1) M^2 i(kU_o - \omega) \hat{d}_o + i(kU_o - \omega) R_o \hat{f}_o = 0, \quad (61)$$

$$\frac{1}{\gamma M^2} T_o \hat{c}_o - \hat{d}_o + \frac{1}{\gamma M^2} R_o \hat{f}_o = 0. \quad (62)$$

Using an elimination process and making use of the following mean flow property relations:

$$\frac{\partial P_o}{\partial y} = 0, \quad \frac{1}{T_o} \frac{\partial T_o}{\partial y} = \frac{1}{R_o} \frac{\partial R_o}{\partial y}, \quad (63)$$

a single differential equation of second order, in terms of the pressure amplitudes, is produced:

$$\frac{\partial^2 \hat{d}_o}{\partial y^2} - \left[\frac{2k}{(kU_o - \omega)} \frac{\partial U_o}{\partial y} + \frac{1}{R_o} \frac{\partial R_o}{\partial y} \right] \frac{\partial \hat{d}_o}{\partial y} - \left[k^2 - \frac{(kU_o - \omega)^2}{A_o^2} \right] \hat{d}_o = 0. \quad (64)$$

Once this equation is solved for \hat{d}_o , the other amplitudes, \hat{a}_o , \hat{b}_o , \hat{c}_o and \hat{f}_o , can be determined in terms of \hat{d}_o . The next step is to obtain the non-trivial solution

of the adjoint problem knowing the eigenvalue, k . The equations defining the components of the adjoint vector are:

$$i\bar{k}R_o\hat{a}_o^* + i(\bar{k}U_o - \omega)R_o\hat{b}_o^* = 0, \quad (65)$$

$$R_o\frac{\partial\hat{a}_o^*}{\partial y} - R_o\frac{\partial U_o}{\partial y}\hat{b}_o^* + i(\bar{k}U_o - \omega)R_o\hat{c}_o^* - R_o\frac{\partial T_o}{\partial y}\hat{d}_o^* = 0, \quad (66)$$

$$i(\bar{k}U_o - \omega)\hat{a}_o^* + \frac{T_o}{\gamma M^2}\hat{f}_o^* = 0, \quad (67)$$

$$i\bar{k}\hat{b}_o^* + \frac{\partial\hat{c}_o^*}{\partial y} - (\gamma - 1)M^2i(\bar{k}U_o - \omega)\hat{d}_o^* - \hat{f}_o^* = 0, \quad (68)$$

$$i(\bar{k}U_o - \omega)R_o\hat{d}_o^* + \frac{R_o}{\gamma M^2}\hat{f}_o^* = 0. \quad (69)$$

Again, using the elimination process and making use of Equations 63, a single differential equation of second order, in terms of \hat{d}_o^* , results in:

$$\begin{aligned} \frac{\partial^2\hat{d}_o^*}{\partial y^2} & \left[\frac{\bar{k}}{(\bar{k}U_o - \omega)^3} \frac{\partial U_o}{\partial y} + \frac{1}{R_o} \frac{\partial R_o}{\partial y} - \bar{k}(\bar{k}U_o - \omega) \frac{\partial U_o}{\partial y} \right] \frac{\partial\hat{d}_o^*}{\partial y} \\ & \left[\frac{2\bar{k}^2}{(\bar{k}U_o - \omega)^2} \left(\frac{\partial U_o}{\partial y} \right)^2 - \bar{k}(\bar{k}U_o - \omega) \frac{\partial^2 U_o}{\partial y^2} \right. \\ & \left. + \bar{k}(\bar{k}U_o - \omega) \frac{\partial U_o}{\partial y} \frac{\partial R_o}{R_o \partial y} + \bar{k}^2 + \frac{M^2 R_o}{(\bar{k}U_o - \omega)^2} \right] \hat{d}_o^* \\ & = 0. \end{aligned} \quad (70)$$

Once this differential equation is solved, the adjoints of the other amplitudes, \hat{a}_o^* , \hat{b}_o^* , \hat{c}_o^* and \hat{f}_o^* , are determined from \hat{d}_o^* . The two differential equations of second order obtained from Equations 64 and 70 can be reduced to two systems of first-order differential equations and solved independently by the use of the Runge-Kutta of order four. The integration is performed along the y -axis for any spanwise location of x . The initial guess used for k is the value obtained by Tam and Block for a shear layer of constant momentum thickness. The integration is started at $y = -\infty$, using the prescribed value of d_o and an arbitrary value of $\partial\hat{d}_o/\partial y$. The integration continues until a value of \hat{d}_o at $y = +\infty$ is obtained. An iteration is performed to yield the value of k such that $\hat{d}_o = 0$ at $y = +\infty$. The process is performed at a number of spanwise locations yielding a numerically defined function, $k(x_1)$. The correction function, $\nu(x_1)$, is then obtained from Equation 54.

PRESENTATION OF RESULTS

In this section, the numerical results of the corrected wave-number, due to the effect of non-parallelism of the shear layer excited by a reflected wave of frequency ω , are presented. These wave-numbers calculated in three different regions of inviscid, outer viscous and fully viscous are matched asymptotically, based on Van Dyke's matching principle, to obtain a uniformly valid result throughout the shear layer region spanning the cavity. In order to find a uniformly valid solution throughout the region for shear layer properties, the set of solutions presented by Equations 55 for the inviscid region and their corresponding equations for regions of outer viscous and fully viscous, respectively, should be matched. These solutions are in terms of the wave-number and their corresponding amplitudes. The constant of integration in the set of solutions for the inviscid region is chosen to be one and that of the outer viscous region is decomposed as $A_o e^{i\phi}$. Part, ϕ , is chosen, such that the wave-number in the two regions of inviscid and outer viscous matches asymptotically. Once the wave-numbers have been matched, the amplitude part in the set of solutions for the inviscid region is matched to its counterpart in the set of solutions for the outer viscous deck on a thin vortex sheet, accordingly, based on Van Dyke's matching principle. By adjusting the time scale between the two foregoing regions, the constant of integration A_o can be determined. The same process is repeated in order to match the shear layer properties, as well as the wave-number between the outer viscous and fully viscous regions.

Here, the following results for different values of wave frequency and Mach number are presented: 1) The corrected wave-number varying along the span of the cavity and its comparison with that of Tam and Block, 2) The instability characteristics of the shear layer at the trailing edge and their comparison with the result of Tam and Block, 3) The tone frequencies predicted by Tam and Block, considering the correction of the wave-number. This result is compared with that of the experimental results of Rossiter.

Figures 3 and 4 show the corrected wave-number varying along the span of the cavity for the case of $\omega = 3.0$, $M = 0.40$ and $M = 0.80$. This clearly shows the dependency of the wave-number/frequency from this study on the spatial coordinate along the span of the cavity. This is opposed to the wave-number/frequency relationship derived in Tam and Block's study, which yields a wave-number that is constant across the cavity for a given frequency. This wave-number, uniformly valid throughout the region of shear layer, has been obtained by matching their corresponding values in the inviscid and viscous regions, based on Van Dyke's asymptotic matching principle, numerically. As the

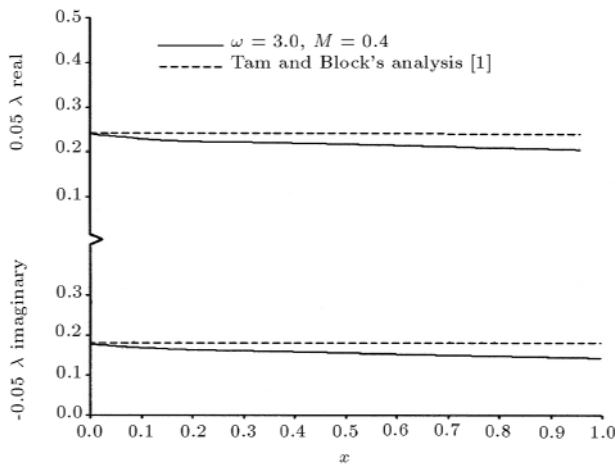


Figure 3. Corrected wave-number for the case of $\omega = 3.0$, $M = 0.4$.

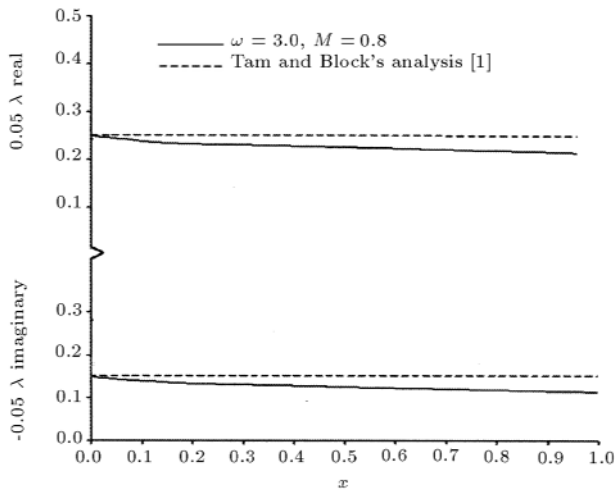


Figure 4. Corrected wave-number for the case of $\omega = 3.0$, $M = 0.8$.

result of this matching, the choice of the perturbation parameter in the outer viscous region, $\varepsilon_1 = \varepsilon^{3/2}$, and in the fully viscous upper deck, $\varepsilon_2 = \varepsilon$, are appropriate. Where the wave-number value in each region intersects the corresponding solution in the adjacent region, it affects the choice of these parameters, which, essentially, are a function of the thickness of the boundary layer in the viscous region. It should be noted that for a given value of the frequency, there is an increase in the value of the wave-number correction function as the Mach number increases.

Figure 5 shows the instability characteristics of the shear layer for the case of $M=0.40$ and its comparison with the analytical result of Tam and Block. Since the author is interested in the temporal instability analysis of the shear layer, the sign of the imaginary part of the wave-number determines the range of instability. If this sign is negative, the shear layer is asymptotically stable and, if positive, the shear layer is

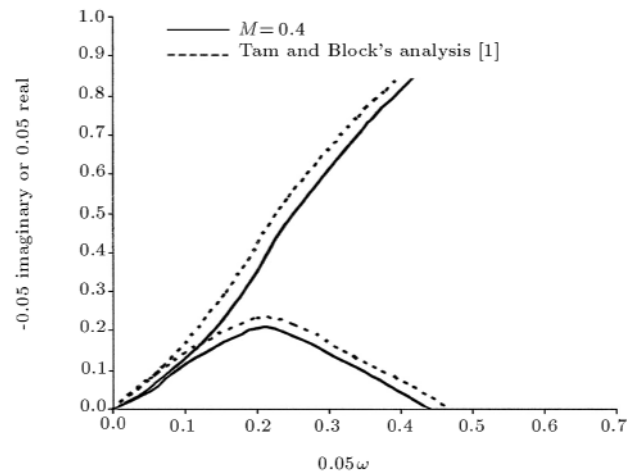


Figure 5. Instability characteristics of shear Layer.

unstable. In Figure 5, the range of unstable frequencies can be clearly identified. It is noted that, in each case, the computations from this study show a reduction in the range of unstable frequencies compared with the analytical result of Tam and Block. A possible explanation is that the viscous effects, considered in the present study but not in Tam and Block's study, have stabilizing effects.

Figure 6 shows the dependence of the Strouhal number of the discrete tone frequencies as a function of Mach number and its comparison with the experimental results of Rossiter [9] for different values of L/D . This calculation is based on $L/D = 4.0$ and $2\theta/L = 0.02$. This figure clearly shows that the Strouhal number of the discrete tone frequencies obtained by the present study indeed provides better agreement with the experimental results of Rossiter. The improvement in agreement of the calculated Strouhal number with Rossiter's data is as much as 22%.

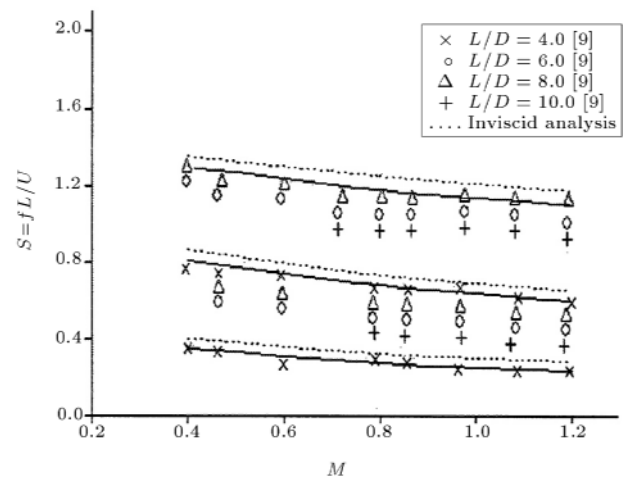


Figure 6. Discrete tone frequencies as a function of Mach number, $L/D = 4.0$ and $Re=100$.

CONCLUSIONS

The analytical results of the wave-number/frequency and instability characteristics of the shear layer for the study of a compressible, viscous flow over an open rectangular cavity, including the effects of shear layer thickness and multiple deck structure on interaction with the trailing edge, have been presented. The result of the work is a comprehensive analysis of the shear layer spanning an open rectangular cavity. Applications may include aircraft weapons bays and wheel wells. For cavities of this nature, the assumption of mean flow inside the cavity is very good. Sound pressure levels inside such cavities can be as high as 150 dB, leading to structural failure and personnel discomfort. It is anticipated that the current work can be used to predict the discrete oscillation frequencies at which the shear layer is excited and, thus, the cavity can be modified such that these frequencies are not excited and the sound pressure level can be reduced. The important parameters in a study of the flow over an open rectangular cavity are the Mach number, the length to depth ratio of the cavity and the Reynolds number. The Reynolds number is important as it is a measure of non-parallel effects in the shear layer. A correlation of these three parameters could be made such that the cavity geometry could be continuously modified to minimize the sound pressure level during the flight. This study could lead to the design of an active controller.

REFERENCES

1. Tam, C.K.W. and Block, P.J.W. "On the tones and pressure oscillations induced by flow over rectangular cavities", *Journal of Fluid Mechanics*, **89**, pp 373-399 (1978).
2. Bartel, A.J. and McAvoy, H.D. "Cavity oscillation in cruise missile aircraft", *Air Force Wright Patterson Aeronautical Laboratories Report, AFWAL-TR-81-3036* (1981).
3. Krishnamurthy, K. "Acoustic radiation from two-dimensional rectangular cut outs in aerodynamic surfaces", *NASA TN-3487* (1955).
4. Gibson, J.F. "An analysis of supersonic cavity flow", Department of Aeronautics and Astronautics, Cambridge, Massachusetts, USA (1958).
5. Spee, B.M. "Wind tunnel experiments on unsteady cavity flow at high subsonic speeds", *Separated Flows*, GARD CP No. 4 (1966).
6. East, L.F. "Aerodynamically induced resonance in rectangular cavities", *Journal of Sound and Vibration*, **3**, pp 75-83 (1966).
7. Smith, D.L. and Shaw, L.L. "Prediction of the pressure oscillations in cavities exposed to aerodynamics flow", *Air Force Flight Dynamics Lab. Report, AFFDL-TR-75-34* (1965).
8. Plumblee, H.E., Gibson, J.S., and Lassiter, L.W. "A theoretical and experimental investigation of the acoustical response of cavities in an aerodynamic flow", United States Air-Force, *WADD-TR-61-75* (1970).
9. Rossiter, J.E. "Wind tunnel experiments on the flow over rectangular cavities at subsonic and transonic speeds", *ARCR7M*, no. 3438 (1969).
10. Smith, D.L. and Shaw, L.L. "Prediction of the pressure oscillations in cavities exposed to aerodynamics flow", *Air Force Flight Dynamics Lab. Report, AFFDL-TR-75-34* (1966).
11. Covert, E.E. "An approximate calculation of the onset velocity of cavity oscillations", *AIAA Journal*, **8**, pp 325-331 (1970).
12. Bilanin, A.J. and Covert, E.E. "Estimation of possible excitation frequencies for shallow cavities", *AIAA Journal*, **11**, pp 369-376 (1973).
13. Block, P.J.W. "Noise response of varying dimensions of subsonic speeds", *NASA Tech. Note D-8351* (1977).
14. Heller, H.H. and Bliss, D.B. "Aerodynamically induced pressure oscillations in cavities-physical mechanisms and suppression concepts", *Air Force Flight Dynamics Lab Report AFFDL-TR-74-133* (1980).
15. Kelly, S.G. "An investigation of compressible flows over open cavities including shear layer thickness effects", *AFOSR Report* (1980).
16. Kelly, S.G. and LaRose, J. "Non-parallel stability of shear layers spanning open cavity", *Bulletin of American Physical Society*, **30**(10), pp 1305-1310 (1985).
17. Colonius, T., Basu, A.J. and Rowley, C.W. "Numerical investigation of the flow past a cavity", *AIAA 99-1912* (1999).
18. Grace, S. "An overview of computational aeroacoustic techniques applied to cavity noise prediction", *AIAA 2001-0510* (2001).
19. Henderson, J., Badcock, K.J. and Richards, B.E. "Understanding subsonic and transonic open cavity flows and suppression of cavity tones", *AIAA 2000-0658* (2000).
20. Rizzetta, D.P. and Visbal, M.R. "Large eddy simulation of supersonic compression-ramp flows", *AIAA-2001-2858* (2001).
21. Shieh, C.M. and Morris, P.J. "Comparison of two- and three-dimensional turbulent cavity flows", *AIAA-2001-0511*, (2001).
22. Stanek, M.J., Raman, G., Kibnes, V., Ross, J., Odedra, J. and Peto, J.W. "Control of cavity resonance through very high frequency forcing", *AIAA 2000-1905* (2000).
23. Stanek, M.J., Raman, G., Kibnes, V., Ross, J.A., Odedra, J. and Peto, J.W. "Suppression of cavity resonance using high frequency forcing- the characteristic signature of effective devices", *AIAA 2001-2128* (2001).

24. Emerson, D.R. and Poll, D.I.A. "High-speed laminar flow over cavities in applications of supercomputers", in *Engr. II., Elsevier, Applied Science Series*, pp 434-441 (1991).
25. Hahn, G. and Drikakis, D. "Large eddy simulation of compressible turbulence using high-resolution methods", *Int. J. of Numerical Fluid Mechanics*, **47**, pp 514-521 (2005).
26. Drikakis, D. "Advances in turbulent flow computations using high-resolution methods", *Progress in Aerospace Sciences*, **39**, pp 603-620 (2003).
27. Saric, S.W. and Nayfeh, A.H. "Non-parallel stability of boundary layer flows", *The Physics of Fluids*, **18**, pp 713-720 (1975).
28. Nayfeh, A.H., *An Introduction to Perturbation Methods*, John Wiley and Sons, New York, USA (1982).
29. Taylor, A.E., *Introduction to Functional Analysis*, John Wiley and Sons, New York, USA (1967).
30. Drazin, P.G. and Reid, W.H., *Hydrodynamic Stability*, Cambridge University Press, Cambridge (1981).